Journal of Geophysical Research: Solid Earth

Supporting Information for

Reexamining the potential to classify lava flows from the fractality of their margins

E. I. Schaefer[1,2], C. W. Hamilton[3], C. D. Neish[1,2], M. M. Sori[4], A. M. Bramson[4], and S. P. Beard[5]

[1] Department of Earth Sciences, University of Western Ontario, 1151 Richmond Street N., London, Ontario, N6A 5B7 Canada

[2] Institute for Earth and Space Exploration, University of Western Ontario, 1151 Richmond Street N., London, Ontario, N6A 5B7 Canada

[3] Lunar and Planetary Laboratory, University of Arizona, 1629 E. University Blvd., Tucson, Arizona, 85721 USA

[4] Department of Earth, Atmospheric, and Planetary Sciences, Purdue University, 550 Stadium Mall Dr., West Lafayette, IN 47907 USA

[5] State Key Laboratory in Lunar and Planetary Science, Macau University of Science and Technology, Avenida Wai Long, Taipa, 999078, Macau

Contents of this file

Introduction

The Supporting Information includes a text section, three figures, and a table. Two figures are provided to clarify points—one geometric and the other interpretive—from the main paper. The text section, with an accompanying figure, describes analyses used to estimate the measurement error. The table reports the results of those analyses.

Text S1.

In the main paper, we estimate that the measurement error for all 15 margin intervals is ~15 cm and attribute that error primarily to unintended tilt of the rover mast. For reference, a tilt of ~4° would apply an offset of 15 cm. In this section, we quantitatively assess that estimate.

For a subset of the ICE-01a margin interval, two rover operators—authors EIS and CDN—each collected vertices independently (Fig. S3). This subset has a straight-line span of 324 m, and the respective along-margin lengths of the two traces are 555 m for EIS and 509 m for CDN. In general, EIS walked the margin more slowly than CDN, which allowed him to walk more closely to the margin and collect finer spatial details than CDN (Fig. S3c). On the other hand, because of her quicker pace, CDN collected most of ICE-01a's length. In the judgement of EIS, these two operators reasonably represent most of the range of inter-operator variability among all operators in the present study.

We take 28 partially overlapping subintervals along the EIS trace, each starting a distance of 15 m along-margin from the previous subinterval. We require each subinterval to have a minimum of 1000 vertices and an along-margin length of at least 150 m. For each such subinterval from the EIS trace, we identify the corresponding subinterval from the CDN trace by proximity. The statistics for both EIS and CDN subintervals are reported in Table S1.

By comparing each CDN subinterval to its EIS counterpart, we can measure directly the precision with which repeated field collection would describe the same margin. This repeatability precision is not identical to measurement error, if that error is interpreted as the discrepancy between the field-collected vertices and the true margin. Nonetheless, we believe an estimate of repeatability precision provides a reasonable estimate of measurement error for our purposes, especially as the trace of the true margin is not independently known. Moreover, EIS generally captured as much spatial detail as any operator, so the EIS trace represents our best estimate of the true margin.

To estimate repeatability precision, we measure the distance from each vertex of each CDN subinterval to the corresponding EIS subinterval. Although only vertices represent the collected data, the fractal analysis method that we use requires interpolation between vertices. Therefore, we include the line segments between vertices as part of the EIS subintervals when calculating distance. Statistics for these distances are reported in Table S1.

A component of these distances is due to translation. As translation has no effect on fractal analysis, it is appropriate to minimize this component and recalculate distances as a better estimate of the relevant measurement error. To minimize systematic offset, we first convert each pair of EIS and CDN subintervals to binary images in which the flow and the area outside the flow are each arbitrarily colored white or black, with a pixel

scale equal to half the median inter-vertex length of that subinterval with the smaller such median. We then use Enhanced Correlation Coefficient Maximization (Evangelidis & Psarakis, 2008) to shift the CDN binary image until its correlation with the EIS binary image is maximized and apply the identified shift to the CDN subinterval to generate CDN′ (Fig. S3c). The distances between CDN′ vertices and EIS subintervals are reported in Table S1.

Most of the translational offset between the EIS and CDN traces is due to the fact that CDN generally maintained a wider berth from the margin than EIS (Fig. S3c). Although this offset is purely translational when individual vertices are considered, the effect at coarser scales is a rescaling. For example, when CDN walked along the perimeter of a lobe, the wider berth would expand the width of that lobe relative to the EIS trace (left side of Fig. S3c). Therefore, the translational component is more dominant at finer scales and is less effectively removed by correlation maximization at the scale of a subinterval, as we have done. The error remaining for CDN′ vertices thus overestimates the error at finer scales, or equivalently, at rod lengths finer than the straight-line span of the subinterval. Among all subintervals, the range of spans is ~68–103 m, and therefore the errors calculated from CDN′ are appropriate for $r \approx 68$ m. The paper focuses on r^* of 1–10 m, which correspond to r of 0.25–40 m. The errors calculated from CDN′ therefore overestimate the error for this this range.

For each of the 28 subinterval pairs, we calculated the mean and median distances between CDN′ vertices and the EIS trace (Table S1). The respective means for these values are 18 cm and 12 cm. We therefore conclude that the estimate of 15 cm for measurement error in the main text is reasonable.

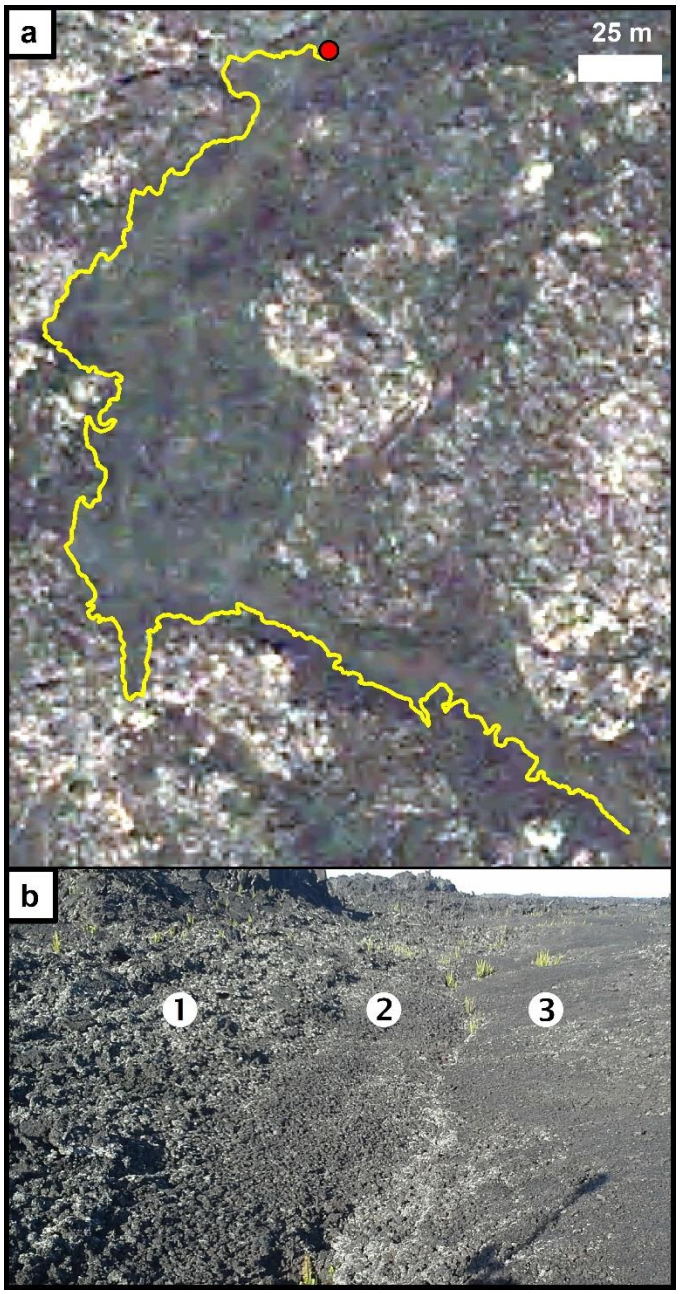

Figure S1. Primary toothpaste lava margin interval HAW-13a and context. (a) HAW-13a (yellow) on same background as Figure 1c of the main text (0.6 m/pixel). North end of HAW-13a (red dot) is location of (b). North is up. (b) Examples of (1) fragmented toothpaste slabs and rubble, (2) a spreading zone, and (3) primary toothpaste lava. View looks east and is not included in HAW-13a.

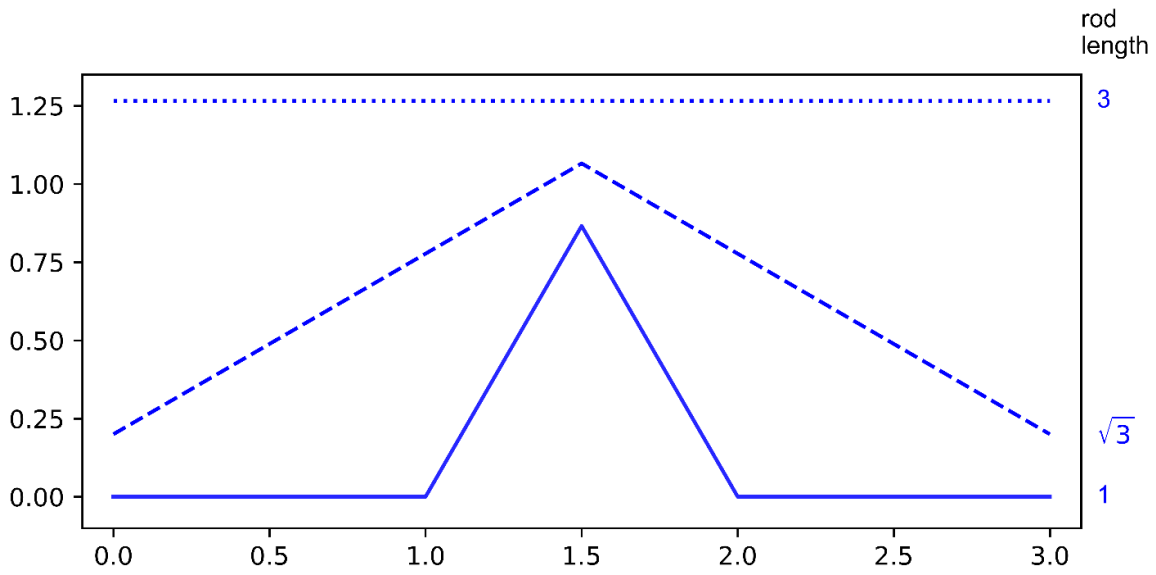

Figure S2. Rod-stepping of motif A (Figure 2a of the main text). The geometries Classic and Random (Figure 2b) are built from motif A (solid line) and its flipped counterpart motif A′ (Figure 2a). The fractal scale-spectra for Classic and Random have a $\sqrt{3}$ periodicity (Figure 2c). This periodicity arises from the three modes in which motif A (and motif A′) can be spanned by rods of different lengths in the divider method (section 3.2.2 of the main text). In their purest forms, the rod length of each mode (solid, dashed, and dotted lines) differs by a factor of $\sqrt{3}$.

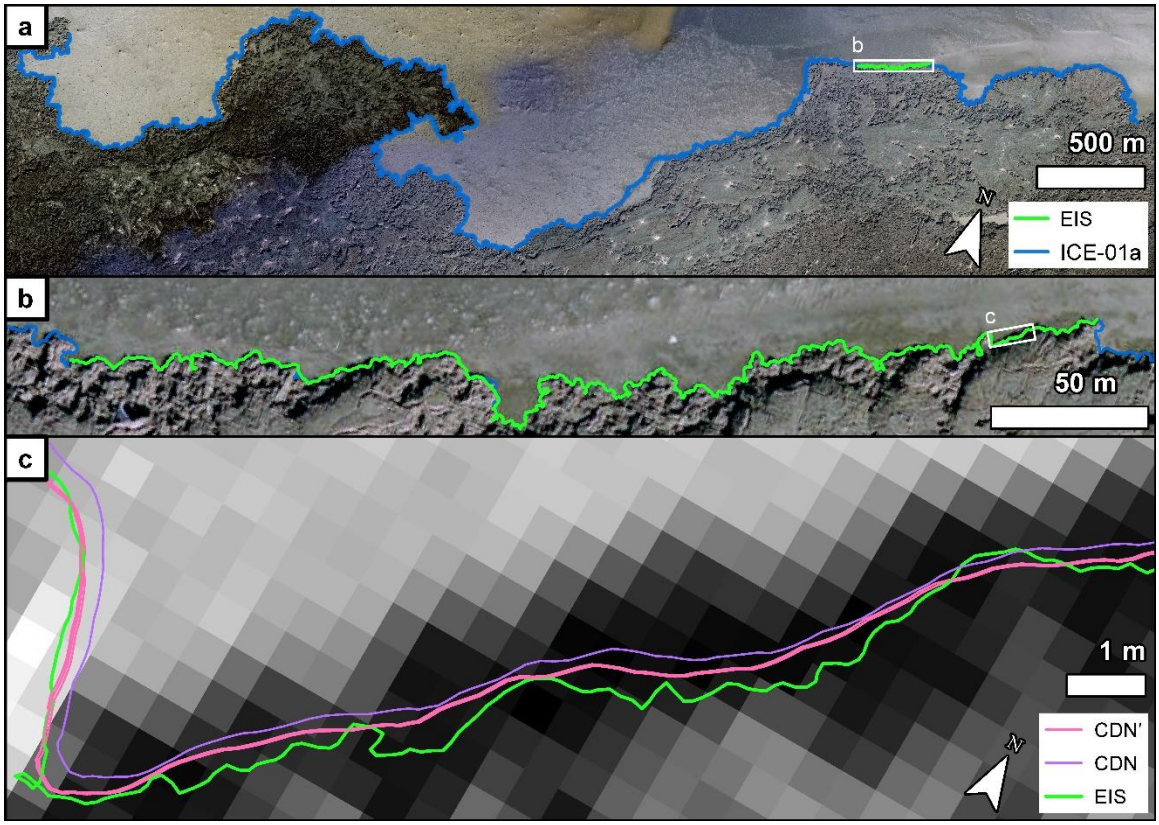

Figure S3. Repeatability precision analysis. Background in each pane is 2015 visible data from Loftmyndir ehf. (0.5 m/pixel). (a) ICE-01a is drawn in blue, and a portion of this margin interval collected by author EIS is superposed and drawn in green. (b) Magnified view of (a). (c) Magnified view of (b), but ICE-01a is not shown. Instead, counterpart intervals collected by authors EIS and CDN are drawn in green and purple, respectively. In addition, subintervals of CDN (CDN′) that have been optimally translated to match counterpart EIS subintervals as nearly as possible are drawn in pink. Background is rendered in grayscale to increase color contrast with the drawn lines.

Table S1

Repeatability Precision Analysis

Subinterval count	28	
Subinterval geometry	EIS	CDN / CDN′
Vertices per subinterval	1000–1071	824–962
Length per subinterval (m)	150–152	133–146
Straight-line span per subinterval (m)	67.9–103	67.5–103
Repeatability precision		
Per-subinterval mean errors	vs. CDN	vs. CDN′
Range (cm)	15–27	13–24
Mean (cm)	22	18
Standard deviation (cm)	3.5	2.5
Per-subinterval median errors	vs. CDN	vs. CDN′
Range (cm)	13–26	10–17
Mean (cm)	18	12
Standard deviation (cm)	4.1	1.8